Applied Catalysis B: Environmental 90 (2009) 105–114

Contents lists available at ScienceDirect

Applied Catalysis B: Environmental

journal homepage: www.elsevier.com/locate/apcatb

Investigation of the NO removal by CO on CuO–CoOx binary metal oxides supported on $Ce_{0.67}Zr_{0.33}O_2$

Lianjun Liu [a], Yu Chen [a], Lihui Dong [a], Jie Zhu [a], Haiqin Wan [a], Bin Liu [a], Bin Zhao [a], Haiyang Zhu [a], Keqin Sun [b,*], Lin Dong [a,*], Yi Chen [a]

[a] Key Laboratory of Mesoscopic Chemistry of MOE, School of Chemistry and Chemical Engineering, Nanjing University, Nanjing, 210093, PR China
[b] Jiangsu Suyuan Environmental Protection Engineering Co. Ltd., No. 58 Su Yuan Road, Jiangning District, Nanjing 211102, PR China

ARTICLE INFO

Article history:
Received 4 November 2008
Received in revised form 5 February 2009
Accepted 25 February 2009
Available online 13 March 2009

Keywords:
CuO–CoOx-CZ catalysts
In situ FT-IR
Interaction
Nitrates

ABSTRACT

Binary metal oxides CuO–CoOx supported on $Ce_{0.67}Zr_{0.33}O_2$ (denoted as CZ, thereafter) catalysts had been characterized by XRD, LRS, UV-DRS, IR, TPR, in situ FT-IR and activity test for the removal of NO by CO. Results suggested that (1) both copper oxide and cobalt oxide (loadings $\leq$0.5 and 0.32 mmol/100 m^2 CZ, respectively) were highly dispersed on CZ support; (2) the addition of cobalt species promoted the reduction of the dispersed copper oxide, and improved the activity of copper oxide supported on CZ due to the strong interaction between active copper oxide and cobalt oxide, which was dependent on the preparation procedure and the cobalt oxide content; (3) the reduction of NO by CO over these catalysts went through different mechanisms at low and high temperatures, which was related to the change of the active species during the reaction process; (4) the introduction of cobalt oxide altered the adsorption type of NO and CO on these catalysts, and oxidized the NO dimers into ionic NO_3^{-1}. A possible reaction mechanism was proposed to discuss the NO + CO reaction based on all these results.

1. Introduction

In the past decades, many researches focused on the selective catalytic reduction (SCR) process to eliminate NOx by ammonia, hydrocarbons, CO and H_2 with the presence or absence of oxygen, using noble metal-containing catalysts. However, these catalysts not only were expensive, but also showed poor thermal stability and resistance to sulfur/phosphate. Hence, transition metal oxides (supported/unsupported) catalysts like CuOx and CoOx had been attempted to replace noble metal-containing catalysts for the SCR process [1–20].

Among them, Co-based catalysts supported on various supports, such as ZrO_2, TiO_2, CeO_2 and γ-Al_2O_3, exhibited the promising activity for CO oxidation [3–5] and NOx reduction [6–20], and the CoOx systems doped with alkali or alkali earth elements had also been employed to the direct decomposition of NO and N_2O molecules [21–26]. The high activity of CoOx (Co_3O_4) seemed to be resulted from the relatively low ΔH of vaporization of O_2 from lattice oxygen atom, which meant that the lattice oxygen was readily to be released at the relative low temperature range. These researchers had paid their primary interests in the relationship between the structure and activity in the De–NOx reaction. For example, He et al. [13] and Liotta et al. [14] investigated the influence of structural and morphological of $CoOx/Al_2O_3/BaO$ catalyst on the catalytic activity for the NO + C_3H_8 and NO + CO reactions, respectively. Indovina et al. [16] studied the dependence of activity and selectivity on sulphate content over CoOx/sulphated-ZrO_2 for the NO abatement with C_3H_6 in the presence of O_2. It was well suggested that the activity and selectivity should be greatly influenced by the concentration of cobalt loading, calcination temperature, precursor and nature of support. However, the Co-based catalysts were less active under SO_2 stream [6], and partially deactivate due to some $CoAl_2O_4$ phase formation or re-aggregation at high temperature and high cobalt content [7,14].

Recently, ceria–zirconia solid solution served as the TWC support had attracted more attention due to its outstanding oxygen storage capacity (OSC) and unique redox properties [2]. As reported elsewhere [1–26] and previously [27–30], it was found that the unitary metal oxide exhibited the suboptimal activity and N_2 selectivity for NO reduction by CO reaction. Unfortunately, few reports could be found about the supported binary metal oxides acting as active species, especially considering cobalt species as modifier, part reasons should be associated with the complex compositions and the interaction of these species. Accordingly, the interaction between binary metal oxides in those catalysts was wide open to study. In addition, the surface adsorbates during the

* Corresponding authors. Tel.: +86 25 83594945; fax: +86 25 83317761.
E-mail addresses: skq1099@yahoo.com.cn (K. Sun), donglin@nju.edu.cn (L. Dong).

0926-3373/$ – see front matter © 2009 Elsevier B.V. All rights reserved.
doi:10.1016/j.apcatb.2009.02.021

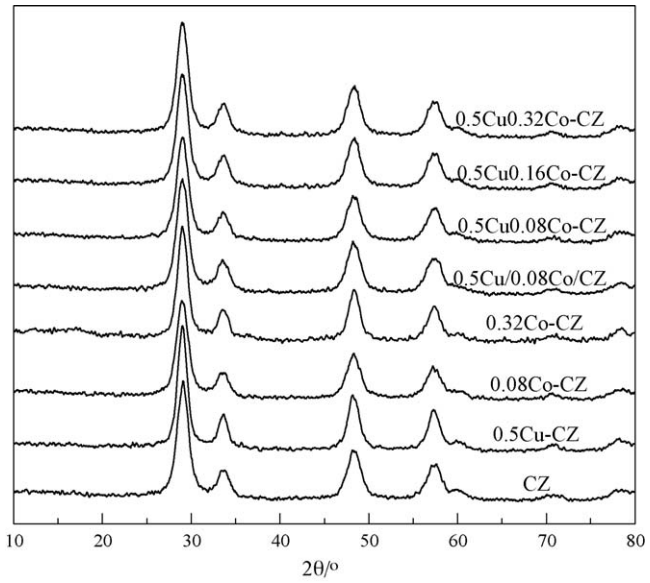

Fig. 1. XRD patterns of CZ support, 0.5Cu-CZ, *y*Co-CZ and *x*CuyCo-CZ catalysts with different CoOx loading amounts.

NO removal process were not clear yet. Along this line, it was expected to combine the advantages of CuO and CoOx by co-impregnating the ceria–zirconia solid solution.

In the present work, the degrees of cobalt dispersion and cobalt–copper interactions were adjusted by varying the cobalt loading and impregnating procedure, our attention was mainly focused on (1) exploring the influence of cobalt oxide species on the catalytic performance of CuO/CZ for NO reduction by CO; (2) investigating the variation of NO or/and CO adsorption over these catalysts at the temperature range 25–350 °C.

2. Experiments

2.1. Catalysts preparation

CZ solid solution was synthesized following the procedure of Li et al. [29]. A requisite amount of $(NH_4)_2Ce(NO_3)_6{\cdot}6H_2O$ and $Zr(NO_3)_4{\cdot}5H_2O$ were dissolved in water, and the excess of ammonia solution was slowly dropped to the mixture solution with vigorously stirring until pH = 10. The resulting solution was kept in stirring for 3 h, aged for 1 h, and then filtered. The obtained solid was dried at 110 °C overnight and then calcined in a muffle stove at 500 °C in flowing air for 4 h. The surface area of CZ was 121.78 m^2/g, which was determined via nitrogen adsorption at 77 K with the Brunauer–Emmet–Teller (BET) method using a Micrometrics ASAP-2000 adsorption apparatus.

The CuO-CZ, CoOx-CZ and CuOCoOx-CZ catalysts were prepared by incipient-wetness impregnating on the support with the solution containing $Cu(NO_3)_2$ or/and $Co(NO_3)_2$. The CuO loading was 0.50 mmol/100 m^2 CZ, while the CoOx was 0.08, 0.16, 0.32 mmol/100 m^2 CZ. The mixture was kept vigorously stirring for 3 h, and then evaporated at 80 °C. The resulting materials were dried at 110 °C overnight and calcined at 500 °C in flowing air for 4 h. These catalysts were denoted as *x*Cu-CZ, *y*Co-CZ and *x*CuyCo-CZ, where the "*x*" and "*y*" indicated the loading amount of copper oxide and cobalt oxide, respectively. In addition, 0.5Cu/0.08Co/CZ catalyst was prepared by stepwise impregnation (first CoOx and then CuO) for comparison under the same condition.

2.2. Catalysts characterization

2.2.1. FT-IR measurement (FT-IR)

FT-IR spectra were collected on a Nicolet 5700FT-IR spectrometer, working in the range of wave numbers 400–4000 cm^{-1} at a resolution 4 cm^{-1} (number of scans, 32). The normal *x*CuyCo-CZ samples were mixed with KBr and pressed into self-supporting disks for IR characterization at room temperature. The IR spectra of CZ support, *x*Cu-CZ, *y*Co-CZ and *x*CuyCo-CZ were obtained by subtracting the KBr spectrum from each specific spectrum. In situ FT-IR spectra for NO or/and CO in IR cell were recorded at various target temperature as background for each test. The *x*CuyCo-CZ catalysts (~10 mg) were mounted in a quarts IR cell and pre-treated for 1 h at 100 °C, followed by the flowing N_2 atmosphere. After cooled to room temperature, the sample wafers were exposed to a controlled stream of CO–N_2 (10% of CO by volume) or/and NO–He (10% of NO by volume) at a rate of 5.0 ml min^{-1} for 30 min. Desorption/reaction studies were performed by heating the adsorbed species at different temperatures. All of the

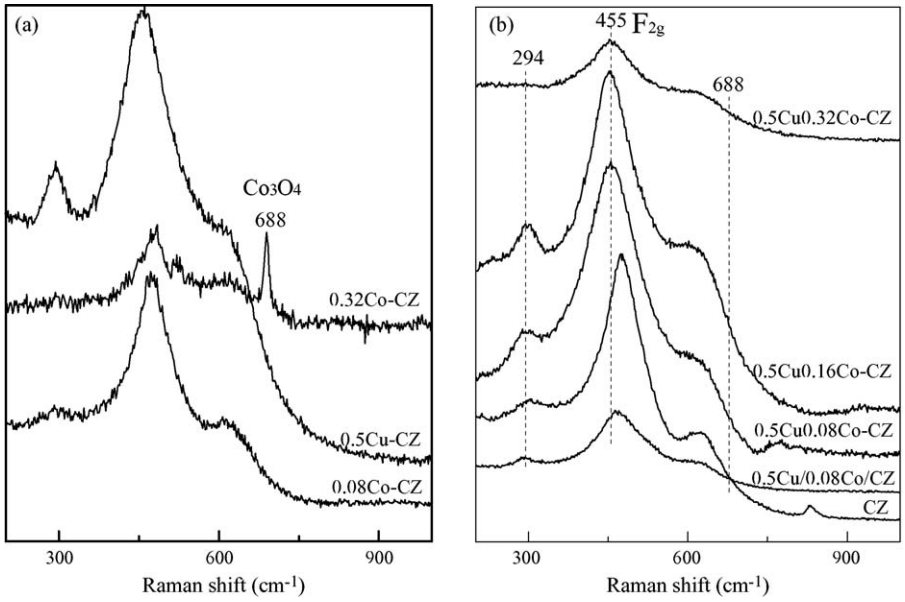

Fig. 2. LRS spectra of these catalysts: (a) 0.5Cu-CZ and *y*Co-CZ; (b) CZ support and 0.5CuyCo-CZ catalysts with different CoOx loading amounts.

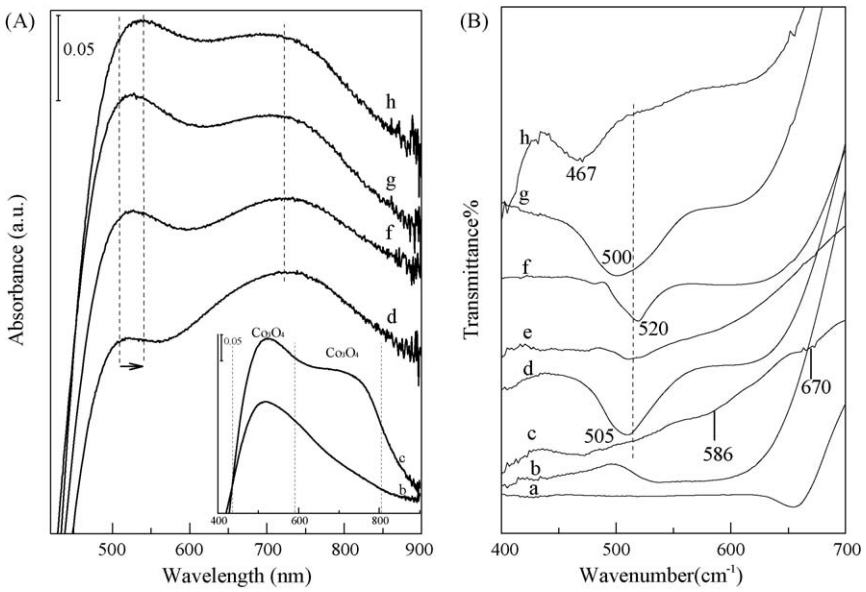

Fig. 3. UV-DRS (A) and IR (B) spectra of these catalysts with different CoOx loading amounts a: CZ; b: 0.08Co-CZ; c: 0.32Co-CZ; d: 0.5Cu-CZ; e: 0.5Cu/0.08Co/CZ; f: 0.5Cu0.08Co-CZ; g: 0.5Cu0.16Co-CZ; h: 0.5Cu0.32Co-CZ.

presented spectra were obtained by subtraction of the corresponding background reference.

2.2.2. X-ray diffraction measurement (XRD)

XRD patterns were recorded on a Philips X'pert Pro diffractometer using Ni-filtered Cu Kα radiation (λ = 0.15418 nm). The X-ray tube was operated at 40 kV and 40 mA.

2.2.3. Laser Raman spectroscopy measurement (LRS)

LRS spectra were collected on a Jobin-Yvon (France-Japa) T64000 type Laser Raman spectroscopy using Ar^+ laser beam. The Raman spectra were recorded with an excitation wavelength of 532 nm and the laser power of 300 mW.

2.2.4. UV–vis diffuse reflectance spectroscopy measurement (UV)

UV–vis DRS spectra were recorded in the range of 200–900 nm by a UV–vis-NIR 5000 spectrophotometer.

2.2.5. H_2-temperature programmed reduction measurement (TPR)

TPR was carried out in a quartz U-tube reactor connected to a thermal conduction detector with H_2–Ar mixture (7.3% H_2 by volume) as reductant. 50 mg of sample was used for each measurement. Before switched to the H_2–Ar stream, the sample was pretreated in a N_2 stream at 100 °C for 1 h. TPR started from room temperature to 550 °C at a rate of 10 °C min^{-1}. These used *x*CuyCo-CZ catalysts were first cooled to room temperature in the flowing N_2, and then quickly transferred to U-tube reactor. The same procedure was then operated for TPR results.

2.3. Catalytic activity tests

The activities of the catalysts were determined under steady state, involving a feed steam with a fixed composition, NO 5%, CO 10% and He 85% by volume as diluents. A quartz U-tube with a requisite quantity of catalyst (50 mg) was used. The catalysts were pretreated in N_2 stream at 100 °C for 1 h and then cooled to room temperature, after that, the gas reactants were switched on. The reactions were carried out at different temperatures with a space velocity of 24,000 h^{-1}. Two volumes and thermal conduction detections were used for analyzing the productions, volume A with Paropak Q for separating N_2O and CO_2, and volume B, packed with 5A and 13X molecule sieve (40–60 M) for separating N_2, NO and CO.

3. Results and discussion

3.1. XRD and Raman results

Fig. 1 showed the XRD patterns of *x*CuyCo-CZ samples. For comparison, XRD results for CZ support and 0.5Cu/0.08Co/CZ samples were also given in Fig. 1. No other diffraction peaks except those for CZ support appeared for all samples, indicating that copper oxide and cobalt oxide (loadings ≤0.5 and 0.32 mmol/100 m^2 CZ, respectively) were highly dispersed on CZ independent of preparation procedure.

The corresponding Raman spectra for these samples were shown in Fig. 2. For 0.32Co-CZ sample, a sharp band at 688 cm^{-1} for the Co_3O_4 species could be detected, which suggested that the cobalt species existed as Co_3O_4 on the CZ support [9,20,32]. However, the Raman spectra of *x*Cu-CZ, *y*Co-CZ and *x*CuyCo-CZ samples were dominated by a strong band at 455 cm^{-1}, which was attributed to the F_{2g} vibration of fluorite-type lattice from CZ support. The band at 294 cm^{-1} was ascribed to tetragonal displacement of the oxygen atoms from their ideal fluorite lattice positions, which was caused by the zirconium ions insertion into ceria lattice [42–44]. For 0.5CuyCo-CZ samples, the main scattering peak of cobalt oxide (Co_3O_4) was absent. This should be due to the interaction between copper oxide and cobalt oxide that led to cobalt oxide well dispersed on CZ, which was supported by XRD results.

3.2. UV-DRS and IR results

Fig. 3A showed the UV-DRS spectra of these *x*CuyCo-CZ catalysts. For 0.32Co-CZ (c), two broad bands at 400–550 and 650–800 nm were presented for the characteristic adsorption of the Co_3O_4 [12]. For 0.5Cu-CZ sample (d), the broad band at 600–850 nm could be ascribed to the adsorption of octahedral Cu^{2+} [28]. Its intensity decreased when cobalt oxide was introduced. While the band at around 520 nm, assigned to the $^4A_2 \rightarrow {}^4T_1$ (4P) transition of Co^{2+} species in tetrahedral coordination [7,10,12,13,15], gradually got stronger and red shifted

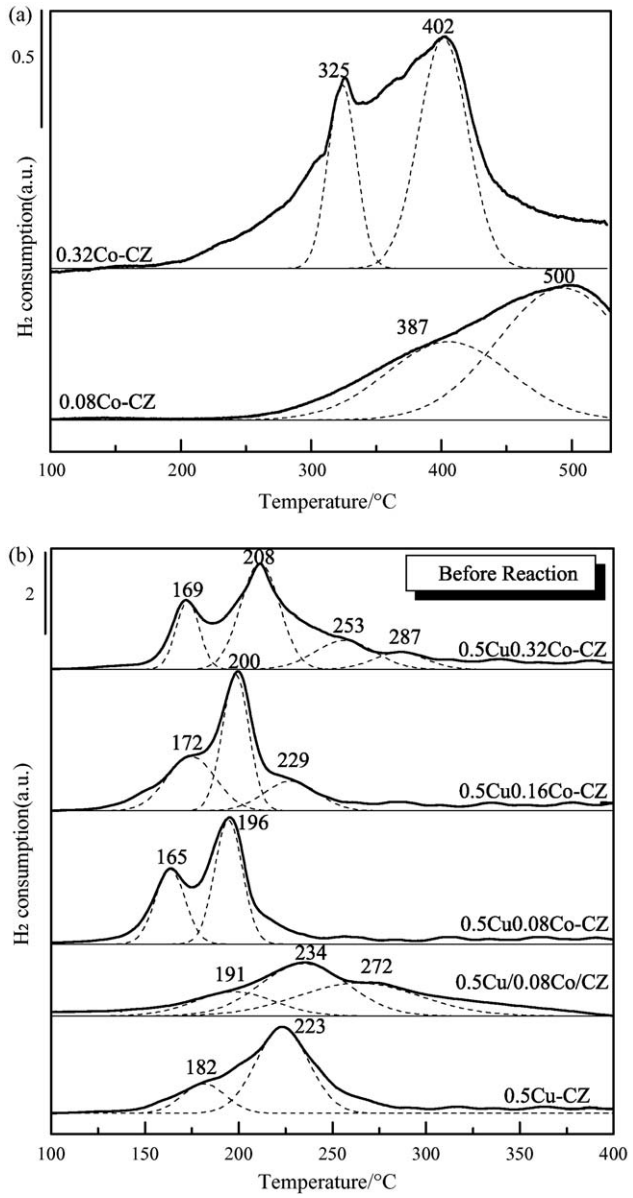

Fig. 4. TPR profiles of H_2 reaction over (a) *y*Co-CZ; (b) 0.5Cu-CZ and *x*CuyCo-CZ catalysts with different CoOx loadings, the 0.5Cu/0.08Co/CZ sample prepared by stepwise impregnation method was also showed in this figure.

with cobalt oxide loadings increasing. The UV-DRS results suggested that the coordination environment of cobalt and copper species was changed due to the strong interaction between them, which was greatly influenced by the content of cobalt oxide.

IR spectra for *x*CuyCo-CZ catalysts and CZ (a) support were shown in Fig. 3B. For both 0.08Co-CZ (b) and 0.32Co-CZ (c) samples, the broad band at 540–580 cm^{-1} and a small one at 670 cm^{-1} can be assigned to the Co–O stretching vibration of cubic spinel Co_3O_4 [13,20], while for 0.5Cu-CZ sample, the peak at 505 cm^{-1} should be attributed to the characteristic vibration of Cu–O bond. For cobalt oxide and copper oxide co-impregnation samples (f–h), the vibration frequency of Cu–O bond shifted from 520 to 467 cm^{-1} when the cobalt content increased from 0.08 to 0.32 mmol/100 m^2 CZ. This shift should be related to the interaction between surface copper oxide and cobalt oxide species. With the cobalt content increasing, more cobalt cations would occupy the surface vacant sites of CZ support and form Cu–O–Co bonds with adjacent copper cations, which resulted in the shift to low frequency [13,31].

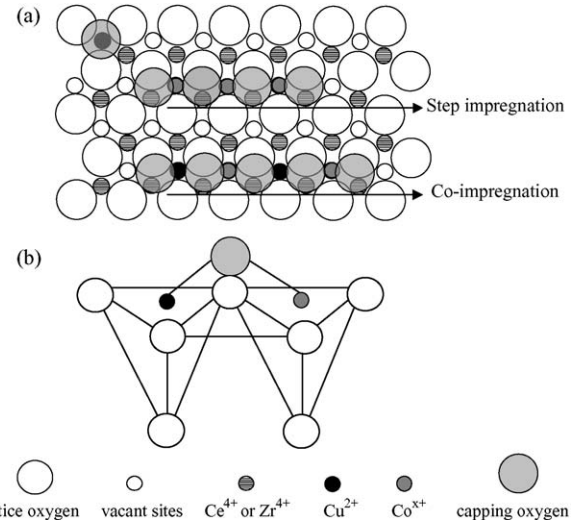

Fig. 5. (a) The schematic diagram of incorporation of the dispersed copper oxide and cobalt oxide on the (1 1 1) plane of the CZ support and (b) the tentative model for the bridging Cu–O–Co bond formation on the (1 1 1) plane of the CZ support.

Consequently, UV and IR results further confirmed that the strong interaction existed between the dispersed copper oxide and cobalt oxide (Co_3O_4) under the current condition.

3.3. Reducible properties of these catalysts (H_2-TPR)

As shown in Fig. 4a, no obvious reduction peak for 0.08Co-CZ in 100–300 °C could be found except a shoulder peak at 387 °C overlapped with the peak at 500 °C, which was due to the higher reduction degree of cobalt oxide at lower temperatures. Regarding 0.32Co-CZ sample, the peak at 325 °C appeared, which should be corresponded to reduction of surface dispersed Co_3O_4 species to CoO, the peak at 402 °C should come from the reduction of CoO to metallic cobalt [4,5,8,9,21,22]. The TPR results of *x*Co-CZ catalysts also replied that Co_3O_4 was formed on the CZ surface after calcinations at 500 °C.

For 0.5Cu-CZ sample (Fig. 4b), the first shoulder at 182 °C and the second broad peak at 223 °C should be the stepwise reduction of dispersed copper oxide groups [1,2,28,29]. For 0.5CuyCo-CZ catalysts, considering no reduction for cobalt oxide below 210 °C, the two reduction peaks in this area were also associated with the stepwise reduction of the dispersed copper oxides. Unlike reduction peaks of 0.5Cu-CZ, they shifted to the lower temperatures with the cobalt oxide loading increasing, suggesting that the introduction of a proper amount of cobalt oxide improved the reducibility of the dispersed copper oxide, which should be related to the strong interaction between surface cobalt oxide and surface copper oxide. For 0.5Cu0.08Co-CZ catalyst, no reduction peak of cobalt oxide appeared, while for 0.5Cu/0.08Co/CZ prepared by stepwise impregnation, the two peaks at 191 and 234 °C were the reduction of surface copper oxide, the third peak at 272 °C should be assigned to reduction of surface cobalt oxide. This might be resulted from the difference of interaction caused by the preparation procedure. According to our report previously [29,30], Fig. 5 showed that the CZ support with fluorite type structure had cubic vacant sites on its (1 1 1) exposed plane. As a result, when the sample was prepared by stepwise impregnation, both dispersed copper oxide and cobalt oxide species were random dispersed on the surface and incorporated into the surface vacant sites, which might lead to the weak interaction between them. However, the Co^{2+} from Co_3O_4 and Cu^{2+} ions with approximate radius could homogeneously occupy these surface positions when prepared by co-impregnation (Fig. 5a), and form bridging Cu–O–Co

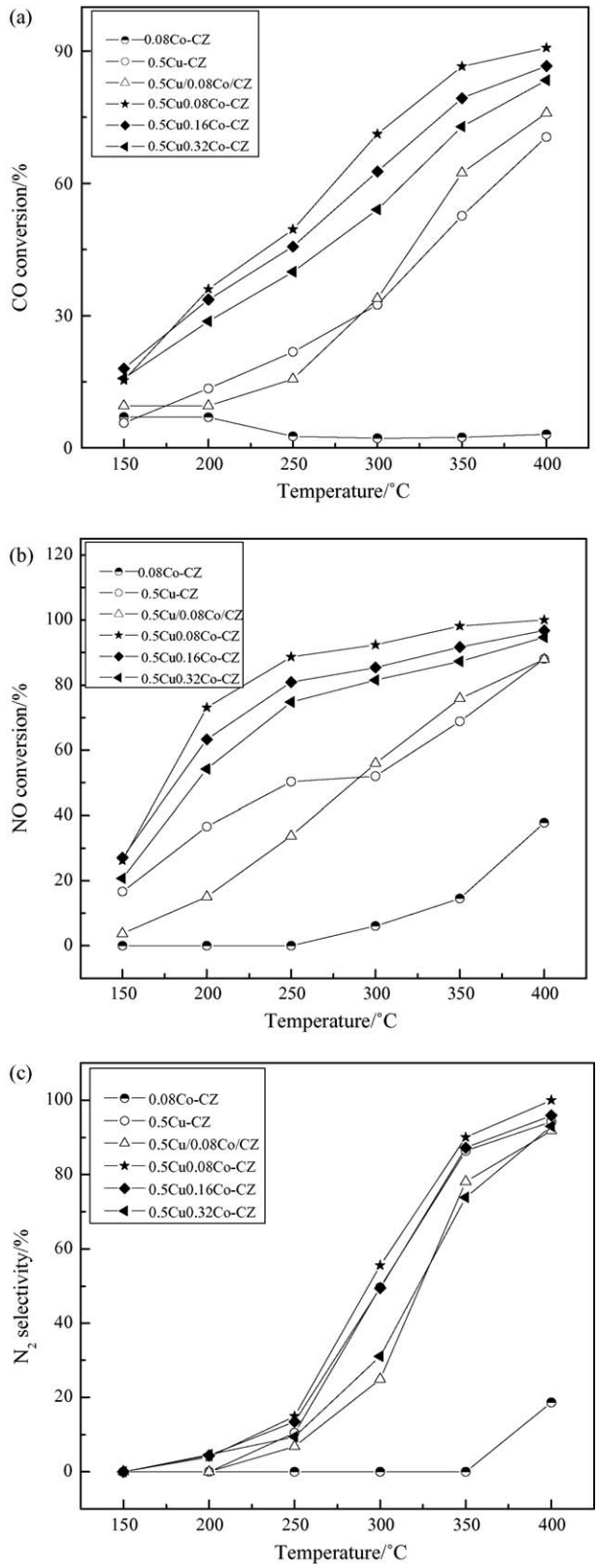

Fig. 6. Results of (a) CO conversion (%), (b) NO conversion (%) and (c) N_2 selectivity (%) over *x*CuyCo-CZ catalysts as a function of reaction temperatures. Feed composition: NO 5%, CO 10% and He 85%, SV = 24,000 h^{-1}.

bond (Fig. 5b), which was supported by UV and IR results. The structure of this bond might be not stable [29] that resulted in the decrease of the reduction temperature of surface copper oxide and surface cobalt oxide.

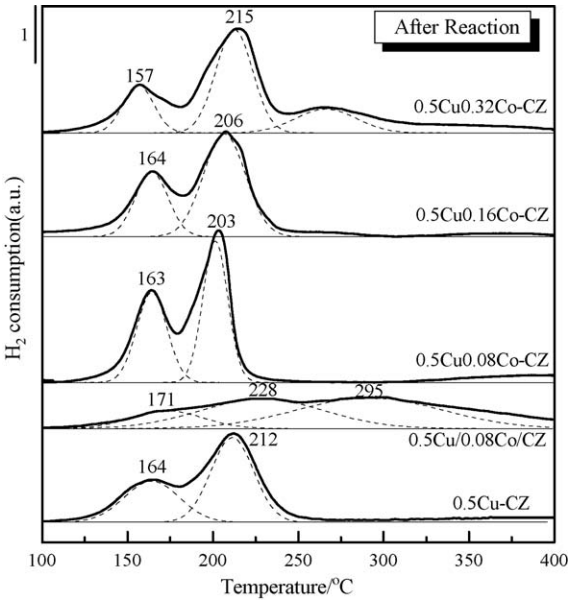

Fig. 7. TPR results for 0.5Cu-CZ, 0.5Cu/0.08Co/CZ and *x*CuyCo-CZ catalysts after reaction at 400 °C.

For 0.5Cu0.16Co-CZ catalyst, the peak at 229 °C was ascribed to the reduction of cobalt oxide. Subsequently, when the cobalt oxide loading reached 0.32 mmol/100 m^2 CZ, two new reduction peaks at 253 and 287 °C appeared, which should also be attributed to stepwise reduction of surface cobalt oxide. Therefore, compared with *x*Co-CZ catalysts, the surrounding copper oxides had also promoted the reduction of surface cobalt oxide, because the neighboring copper oxides could weaken the strength of Co–O bond and promote desorption of lattice oxygen from Co_3O_4 [4,8,9]. On the other hand, since the reduction of Cu^{2+} to metallic Cu occurred at about 220 °C, the formation of Cu could enable the spill-over hydrogen from metal to reduce cobalt oxide, thus the reduction temperature of cobalt oxide decreased. This similar promotion effect for the reduction of ceria by cobalt was reported by Li et al. [22].

3.4. Catalytic activity and selectivity of NO reduction by CO

Fig. 6 gave the CO/NO conversions and N_2 selectivity of *x*CuyCo-CZ catalysts for the NO removal by CO reaction as a function of temperature. Both the CO/NO conversion and N_2 selectivity increased with the temperatures. As displayed in Fig. 6a and b, the 0.08Co-CZ catalyst showed negligible activity below 350 °C, while 0.5Cu-CZ catalyst exhibited 20–50% in CO and NO conversion below 350 °C. Hence, regarding all the catalysts, copper oxide species were considered as the main active species below 350 °C. When the cobalt oxide was introduced into the 0.5Cu-CZ sample, the CO and NO conversions below 350 °C changed greatly depending on the preparation procedure and cobalt loading. For cobalt oxide preloaded sample, i.e. 0.5Cu/0.08Co/CZ, the CO and NO conversions decreased with the introduction of cobalt oxide; while for the co-impregnation sample, i.e. 0.5Cu0.08Co-CZ, the CO and NO conversions were enhanced significantly. However, for 0.5CuyCo-CZ samples, the enhancement decreased slightly with cobalt oxide content increasing, which should be due to the active particles agglomeration [6–8,14–16]. Shu et al. [39] found that the catalytic activity for NO reduction by CO over CuO/Co_3O_4 decreased after the molar ratio of copper and cobalt species achieved a certain value. They proposed that different copper oxide content probably resulted in different dispersion of copper oxide and

Table 1
The peak area of H_2 relative consumption for these catalysts before and after reaction.

Samples	0.5Cu-CZ	0.5Cu/0.08Co/CZ	0.5Cu0.08Co-CZ	0.5Cu0.16Co-CZ	0.5Cu0.32Co-CZ
BR H_2 RC (a.u.)	116.31	135.10	146.53	190.64	211.54
AR H_2 RC (a.u.)	86.30	84.36	97.27	86.76	112.75

H_2 RC: H_2 relative consumption; BR: before reaction; AR: after reaction.

changed the active sites on the surface of catalysts. These results suggested that the catalytic activity of these catalysts was influenced by the preparation procedure and cobalt oxide content. The co-impregnation samples gave better activity than that of cobalt oxide preloaded samples. In the present work, the optimal cobalt oxide content was 0.08 mmol/100 m^2 CZ.

In addition, these catalysts exhibited very low N_2 selectivity below 300 °C, and the high selectivity was achieved dramatically when the temperature was above 300 °C. In comparison with 0.5Cu-CZ, 0.5Cu0.08Co-CZ catalyst slightly enhanced the N_2 selectivity. However, the N_2 selectivity gradually decreased over 0.5Cu0.16-CZ and 0.5Cu0.32Co-CZ catalysts. In a word, this could be explained considering that the cobalt oxide was easily aggregated at high content, thus rendering the relevant samples non-selective for NO reduction. These results revealed that N_2O formation was favored during the initial stage (≤300 °C) and N_2

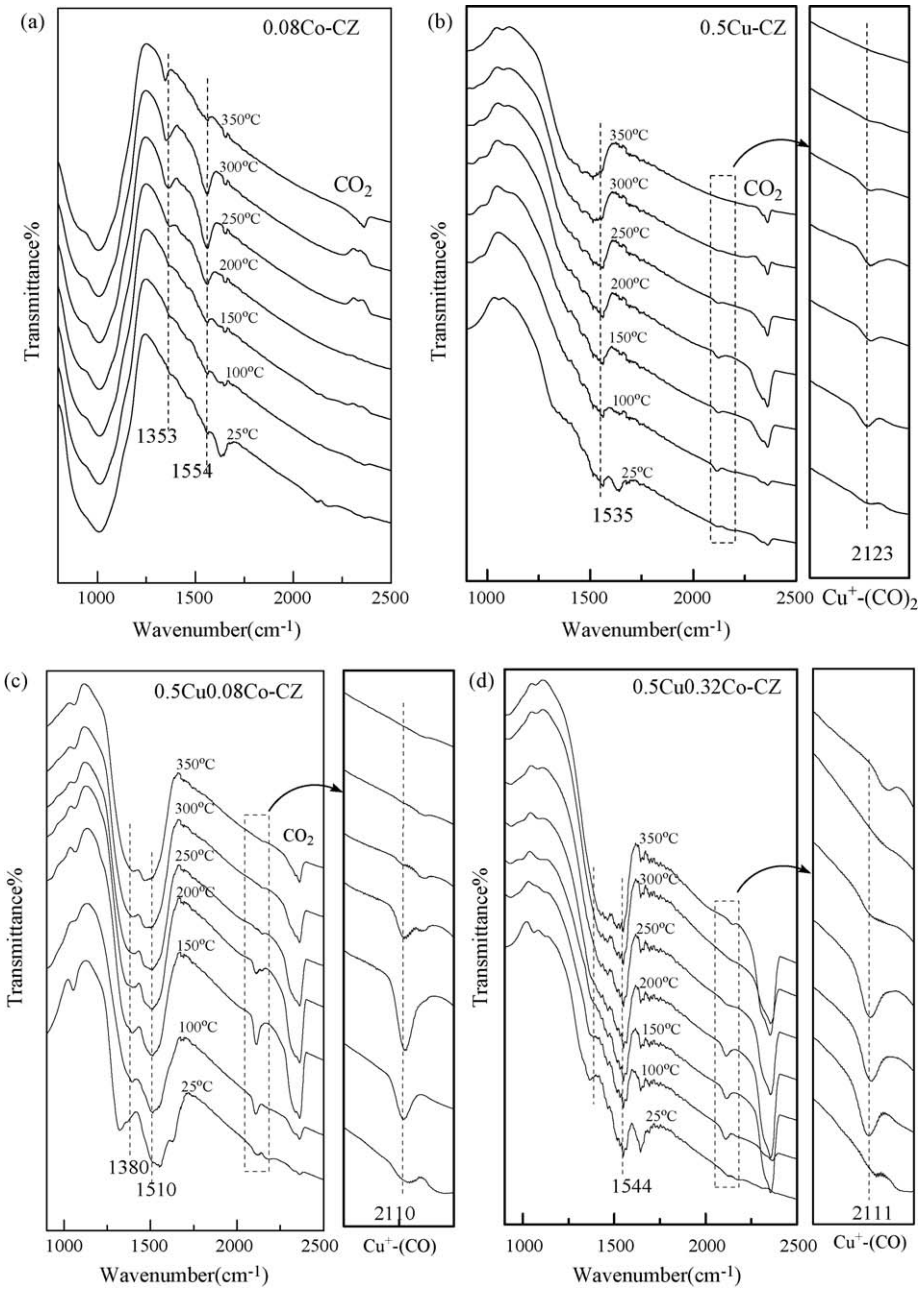

Fig. 8. In situ FT-IR results of CO (10% in volume) adsorption on *x*CuyCo-CZ catalysts from 25 to 350 °C at a heating rate of 10 °C min^{-1}. (a) 0.08Co-CZ; (b) 0.5Cu-CZ; (c) 0.5Cu0.08Co-CZ; (d) 0.5Cu0.32Co-CZ.

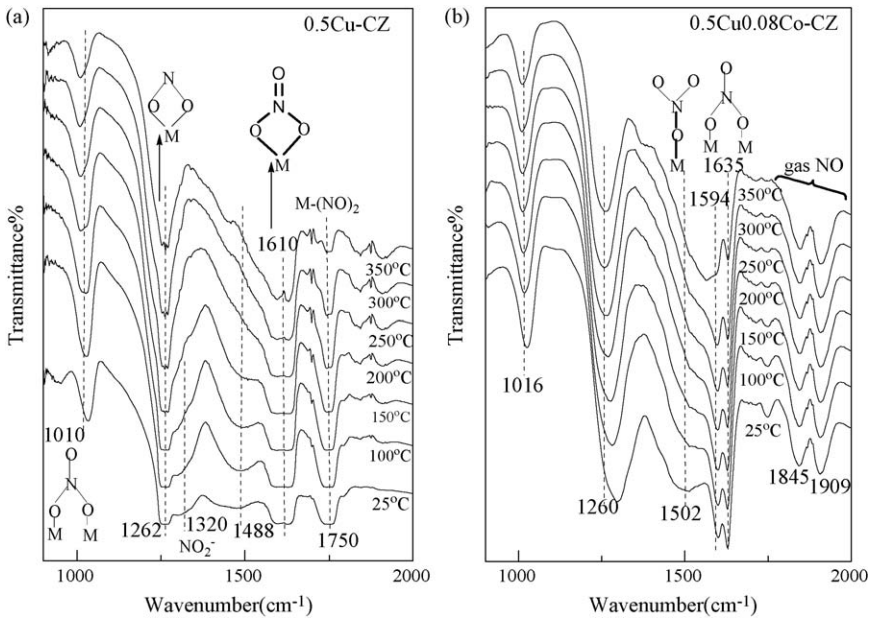

Fig. 9. In situ FT-IR results of NO (10% in volume) adsorption on *x*CuyCo-CZ catalysts from 25 to 350 °C at a heating rate of 10 °C min^{-1}. (a) 0.5Cu-CZ; (b) 0.5Cu0.08Co-CZ.

was mainly produced at the subsequent process (>300 °C) [21,25,41]. Liotta et al. [14] also reported that NO reduction by CO occurred with different selectivity to N_2O/N_2 at different temperature range over Co/Al_2O_3-BaO catalyst.

Generally, it was accepted that finely dispersed surface Co^{2+} ions were active and selective for NO reduction and tetrahedral Co^{2+} ions in $CoAl_2O_4$ spinels were inactive, whereas Co_3O_4 particles catalyzed the decomposition of N_2O and the combustion of hydrocarbons [9,10,13,14,26]. The Cu^{2+}/Cu^+ or Cu^+/Cu^0 redox couples were found to be effective for selectively catalytic reduction of NO by CO [1,28,38]. As previously established for unsupported or supported copper-cobalt spinels catalysts, the formation of Cu^{2+}–Co^{3+} ions pairs played the decisive role for the activity towards NO + CO reaction [38-41]. In the present study, taking into account of the LRS, IR, UV and TPR results, it was inferred that the interaction between copper oxide and cobalt oxide might affect the oxidation state of copper oxide and cobalt oxide via the reaction of $Cu^{2+} + Co^{2+} \leftrightarrow Cu^+ + Co^{3+}$, which was dependent on the cobalt content and preparation procedure. Thus the synergistic effect between copper oxide and cobalt oxide would greatly improve the activity. On the other hand, this reaction possibly went through different mechanisms at low and high temperatures due to the change of active species during the reaction process. Fig. 7 showed the TPR results for these catalysts after reaction at 400 °C, the reduction features were similar to that of samples before reaction, and the reduction temperatures for the second peaks increased. The peak area of H_2 consumption for these samples was also calculated, as listed in Table 1. It is found that the peak area of H_2 consumption for these used catalysts decreased compared with that of before reaction, which revealed that partial copper and cobalt oxides were reduced to the low valence state by CO. Moreover, for 0.5Cu0.16Co-CZ sample, the reduction peak for surface cobalt oxide disappeared or overlapped with the dispersed copper oxide, while for 0.5Cu0.32Co-CZ sample, there was just one peak at 267 °C for cobalt oxide reduction. This result suggested that the Co_3O_4 should be reduced into CoO after reaction at high temperature, while Co^{2+} ions were selective for NO reduction to N_2 [14,23]. The change of active species resulted in the enhancement of N_2 selectivity above 300 °C.

3.5. CO or/and NO interaction with xCuyCo-CZ catalysts

3.5.1. CO interaction with xCuyCo-CZ catalysts

Fig. 8 showed in situ FT-IR results of CO interaction with *x*CuyCo-CZ catalysts as the temperature increasing from 25 to 350 °C. For 0.08Co-CZ sample in the CO flow, two bands at 1353 and 1554 cm^{-1} assigned to surface carbonate species [5,7] appeared, and their intensity got stronger when the temperature increased to 250 °C. Then the temperature was raised further to 350 °C, these two bands got smaller due to their decompositions. At the same time, a new peak at 2360 cm^{-1} was present, which was attributed to the adsorption of CO_2. These results suggested that surface cobalt oxide was reduced by CO at around 350 °C. Correspondingly, for 0.5Cu-CZ sample, the bands at 1535 and 2123 cm^{-1} appeared below 300 °C, which should be ascribed to the surface carbonates and Cu^+–$(CO)_2$ species, respectively. Meanwhile, the trace of CO_2 (2360 cm^{-1}) could be detected. These results suggested that copper oxide species were ready to be reduced to Cu^+ by CO. For 0.5Cu0.08Co-CZ and 0.5Cu0.32Co-CZ samples, a band at 2110 cm^{-1} could be obtained at room temperature, which should be ascribed to the adsorption of linear CO–Cu^+ species [27], indicating that CO altered its adsorption type on Cu^+ ions when cobalt oxide was introduced into the catalysts. When the temperature was raised to 300 °C, all CO adsorption species on Cu^+ essentially disappeared, which might be resulted from the reduction of Cu^+ ions to Cu metal. Considering the activities of these catalysts, the main active species in these catalysts below 300 °C were Cu^{2+}/Cu^+ species, which had a low N_2 selectivity; when the temperature was higher than 300 °C, the main active species were Cu^+/Cu^0 species, which had a high N_2 selectivity. Li et al. [22] concluded that addition of CeO_2 promoted the reduction of Co^{3+} to Co^{2+} by facilitating the desorption of adsorbed oxygen species, which was the rate-determining step of N_2O decomposition. Similarly, the introduction of cobalt oxide could promote the reduction of Cu^{2+} to Cu^+ by their strong interaction as well as the reduction of Co_3O_4 at high temperature by copper oxide and CZ support, which could synergistically enhance the activity and N_2 selectivity. Herein, these experiments further corroborated the TPR and activity test results.

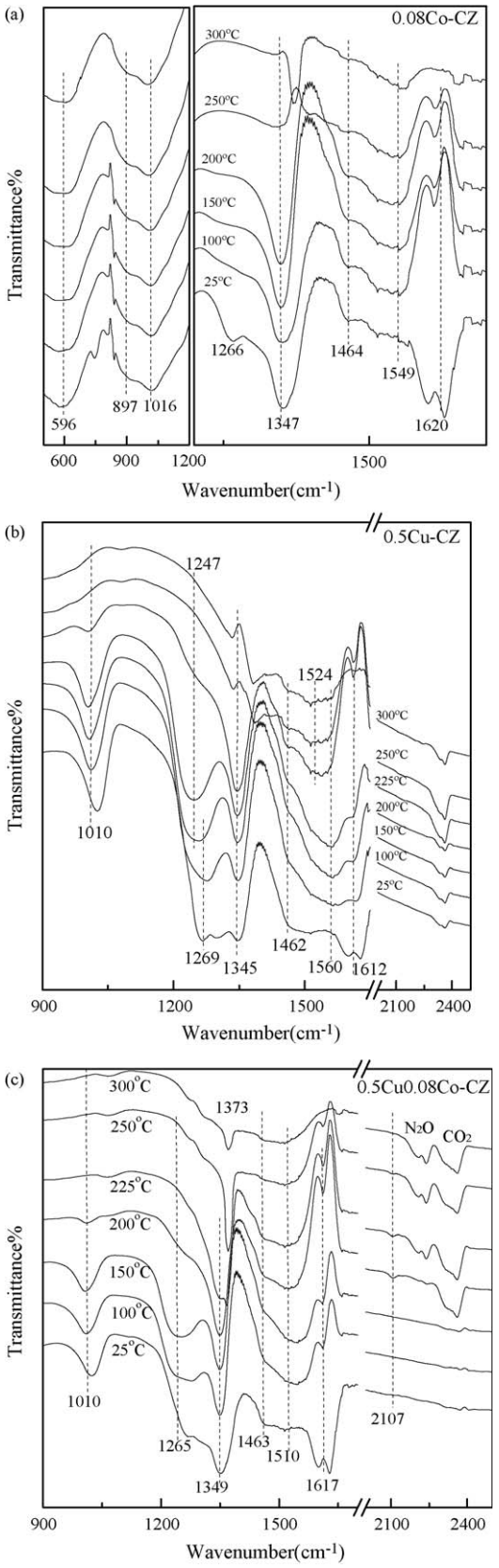

Fig. 10. In situ FT-IR results of NO and CO (10% in volume, respectively) co-adsorption on *x*CuyCo-CZ catalysts with changing temperature from 25 to 300 °C at a heating rate of 10 °C min^{-1}. (a) 0.08Co-CZ; (b) 0.5Cu-CZ; (c) 0.5Cu0.08Co-CZ.

Table 2
Assignment and the desorption temperature of these FT-IR bands for NOx species during the interaction of NO and CO mixture with the catalysts from 25 to 300 °C.

The adsorbed	Bands position (cm^{-1})			Desorption temperature (°C)		
NOx species	a	b	c	a	b	c
Bridging nitrate	1620	1612	1617	100	225	100
Monodentate	1464	1462	1463	250	>300	250
Bidentate nitrate	1016	1010	1010	>300	250	225
Chelating nitrite	1266	1269, 1247	1265	100	250	200
Nitrate ions	1372	–	1373	>300	–	300
Bridging nitro	1549	1560	1510	>300	>300	300
Cis-$N_2O_2^{2-}$	1347	1345	1349	300	250	250
N_2O	–	–	2230	–	–	>300
Cu^+–CO	–	–	2107	–	–	300

a: 0.08Co-CZ; b: 0.5Cu-CZ; c: 0.5Cu0.08Co-CZ.

3.5.2. NO interaction with xCuyCo-CZ catalysts

In order to obtain the information of the adsorbed NO species on 0.5Cu-CZ and 0.5Cu0.08Co-CZ, the NO adsorption FT-IR spectra of these two catalysts had been recorded, as shown in Fig. 9. For 0.5Cu-CZ sample, the bands at 1320 and 1488 cm^{-1} could be attributed to the monodentate nitrite NO_2^{-1} and the asymmetrical stretching variation of monodentate NO_3^{-1}, respectively [10,17]. These bands disappeared at 200 °C due to their poor stability. The bands for chelating nitrite at 1262 cm^{-1}, the bidentate NO_3^{-1} at 1010 and 1610 cm^{-1} and the M–$(NO)_2$ [19] at 1750 cm^{-1} could also be observed even when the temperature was raised to 350 °C, indicating they were stable at current condition. While for 0.5Cu0.08Co-CZ sample, neither monodentate nitrite NO_2^{-1} nor M–$(NO)_2$ was present. The band attributed to the adsorption of monodentate nitrate had shifted from 1488 to 1502 cm^{-1} as well as bidentate nitrate from 1610 to 1594 cm^{-1}. The desorption temperature increased from 200 to 300 °C when cobalt oxide was added. This might be due to the strong interaction between NO and surface cobalt species [18]. A new band at 1635 cm^{-1} was observed, which belonged to the adsorption of bridging bidentate nitrate that was stable even at 350 °C. These results disclosed that the introduction of cobalt oxide also influenced the adsorption type of NO on these catalysts due to the change of charge balance. This was caused by the interaction between the dispersed cobalt oxide and copper oxide. Moreover, compared with single copper oxide, the chemisorbed NO at 1830 and 1910 cm^{-1} could be observed at room temperature and maintain identical in the whole process. As reported elsewhere, these bands were assigned to the symmetric and asymmetric stretching modes of Co^{2+}–NO or ON–Co^{2+}–NO_2^{-1} complexes [15,17]. On the whole, the introduction of cobalt oxide had significantly provided new sites for NO adsorption.

3.5.3. NO and CO co-interaction with xCuyCo-CZ catalysts

FT-IR for NO and CO co-interaction had been performed to further approach the NO + CO reaction mechanism over the catalyst surface in the temperature range of 25–300 °C. After exposure these catalysts to the reactants mixture at room temperature, NO preferentially interacted with the active sites and formed several kinds of nitrite/nitrate like species. As shown in Fig. 10a, the band at 1266 cm^{-1} for chelating nitrite and the band at 1620 cm^{-1} for bridging bidentate nitrate on 0.08Co-CZ surface disappeared at 100 °C, whereas the band at 1347 cm^{-1} for cis-$N_2O_2^{2-}$ [33] was more thermally stable and more intense with temperature increasing. The similar behaviors were observed for monodentate nitrate at 1464 cm^{-1} and bridging nitro at 1549 cm^{-1} [9,10,17,18]. When the temperature increased to 300 °C, those bands for nitric oxide adsorption species in the region 1200–1700 cm^{-1} disappeared except the band at 1549 cm^{-1} for bridging nitro species. At the same

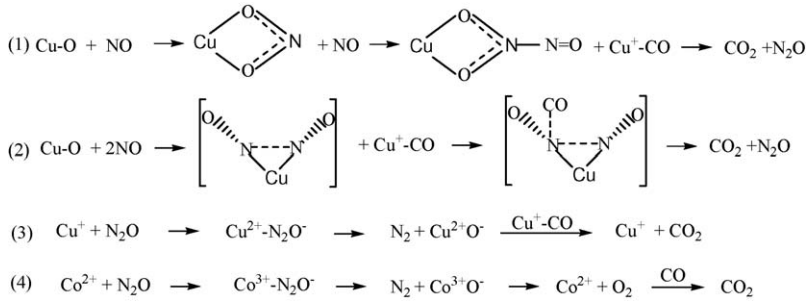

Fig. 11. Possible schemes for adsorbed NO reduction by CO over *x*CuyCo-CZ catalysts.

time, the band for nitrate ion at 1372 cm^{-1} appeared, which should be from the cis-$N_2O_2^{2-}$ oxidized by oxygen form Co-CZ. For 0.5Cu-CZ sample, the band at 1560 cm^{-1} for bridging nitro gradually grew up at the expense of the bands at 1612 cm^{-1} for bridging nitrate and 1462 cm^{-1} for monodentate nitrate disappearance. While the band at 1269 cm^{-1} shifted to 1247 cm^{-1} due to the reform of linear NO_2^- to chelating nitrite [10,33]. When the temperature reached 250 °C, the strong band at 2360 cm^{-1} for CO_2 appeared and those bands for adsorbed nitrite oxide species disappeared, indicating that these species including chelating nitrite, cis-$N_2O_2^{2-}$, monodentate, bidentate and bridging nitrate had reacted with CO molecules.

Interestingly, for 0.5Cu0.08Co-CZ sample, the band at 1010 cm^{-1} for bidentate nitrate and the band at 1265 cm^{-1} for chelating nitrite were synchronously dissolved at 200 °C, while the band at 1349 cm^{-1} for cis-$N_2O_2^{2-}$ and the band at 1463 cm^{-1} for monodentate nitrate vanished at 225 °C. Subsequently, the free ionic NO_3^{-1} at 1373 cm^{-1} prominently dominated the whole reaction. The band for bridging nitro had shifted from 1560 to 1510 cm^{-1}, and was gradually weakened with increasing temperature. During the heating process, the N_2O at 2230 cm^{-1} [19] and CO_2 at 2360 cm^{-1} were distinctly observed from the IR spectra at 150 °C, which suggested they were products originating from CO reaction with these adsorbed NOx intermediates. In addition, a weak band at 2107 cm^{-1} for CO bonded to Cu^+ [27] was also represented at 200 °C and disappeared at 300 °C, which should be resulted from the stepwise reduction of surface copper oxide by CO. The assignment and the desorption temperature of these adsorbed NOx species were summarized in Table 2. These results suggested (1) the introduction of cobalt oxide decreased the active temperature of these catalysts; (2) the active species should be changed at high temperature and (3) the NO removal by CO would go through different mechanisms below and above 300 °C, which was supported by activity tests. As reported elsewhere, NO and CO preferentially adsorbed on Cu^{2+} sites and Cu^+ sites, respectively, when NO and CO co-existed in gas phase over highly loaded CuO [1]. In other words, the addition of cobalt species had promoted Cu^+ creation from the dispersed Cu^{2+}. N_2 was formed via the reaction of N_2O with Cu^+–(CO), while the reduced cobalt oxide might play an important role in decomposing the NO/N_2O at high temperature [1,17,34].

On the basis of the literatures and our present works, a possible reaction mechanism was proposed for NO reduction by CO over these catalysts. As shown in Fig. 11, it was assumed that NO was preferentially adsorbed on dispersed copper oxide or oxygen vacancy sites of CZ below 300 °C. Eqs. (1) and (2) showed the adsorbed NO species, i.e. chelating nitrite and cis-$N_2O_2^{2-}$. These adsorbates reacted with CO activated by Cu^+ species and produced N_2O and CO_2, which was in agreement with the similar reports [34,35,37]. Similarly, according to Taniike et al. theoretic calculations [36], the NO dimers for cis-$N_2O_2^{2-}$ should be favored to form N_2O over cobalt sites. When the temperature was higher than 300 °C, the catalyst might be reduced by CO, namely Cu^+ and Co^{2+} ions, which were selective to N_2 in the catalytic removal of NO by CO [13,14,26]. The main Cu^+ species should contribute to the N_2O reduction by CO, while the dispersed cobalt oxide should play an important role in N_2O decomposition and reduction by CO, as given in Eqs. (3) and (4).

4. Conclusions

Both copper oxide and cobalt oxide (Co_3O_4) were highly dispersed on ceria–zirconia solid solution. The introduction of cobalt oxide had significantly improved the activity of NO reduction by CO over copper oxide supported on CZ, and also promoted the reduction of dispersed copper oxide due to the strong interaction between the copper oxide and cobalt oxide species, which was dependent on the preparation procedure and cobalt oxide content.

CO or/and NO adsorption FT-IR results showed that the introduction of cobalt species had facilitated the production of Cu^+ species under the CO atmosphere and influenced the adsorption type of CO and NO. Besides, the addition of cobalt oxide oxidized the NO dimers for cis-$N_2O_2^{2-}$ into ionic NO_3^{-1}. During the reaction process, partial surface active species might be reduced into low valence state above 300 °C, as evidenced by TPR and in situ FT-IR results. This reaction possibly went through different mechanisms at low and high temperatures over *x*CuyCo-CZ catalysts due to the change of active species.

Acknowledgement

The financial supports of the National Natural Science Foundation of China (No. 20873060) and the National 973 Program of China (No.2004CD719502) are gratefully acknowledged.

References

[1] F. Amano, S. Suzuki, T. Yamamoto, T. Tanaka, Appl. Catal. B: Environ. 64 (2006) 282–289.
[2] L. Ma, M.F. Luo, S.Y. Chen, Appl. Catal. A: Gen. 242 (2003) 151–159.
[3] W.H. Yang, M.H. Kim, S.W. Ham, Catal. Today 123 (2007) 94–103.
[4] C.W. Tang, M.C. Kuo, C.J. Lin, C.B. Wang, S.H. Chien, Catal. Today 131 (2008) 520–525.
[5] M.M. Yung, Z.K. Zhao, Z.K. Zhao, M.P. Woods, U.S. Ozkan, J. Mol. Catal. A: Chem. 279 (2008) 1–9.
[6] M.F. Irfan, J.H. Goo, S.D. Kim, Appl. Catal. B: Environ. 78 (2008) 267–274.
[7] D. Pietrogiacomi, S. Tuti, M.C. Campa, V. Indovina, Appl. Catal. B: Environ. 28 (2000) 43–54.
[8] L.F. Liotta, G. Pantaleo, A. Macaluso, G.D. Carlo, G. Deganello, Appl. Catal. A: Gen. 245 (2003) 167–177.
[9] L.B. Gutierrez, E.E. MirÓ, M.A. Ulla, Appl. Catal. A: Gen. 321 (2007) 7–16.
[10] F.X. Zhang, S.J. Zhang, N. Guan, E. Schreier, M. Richter, R. Eckelt, R. Fricke, Appl. Catal. B: Environ. 73 (2007) 209–219.
[11] T. Maunula, J. Ahola, H. Hanmada, Appl. Catal. B: Environ. 26 (2000) 173–192.
[12] J.C. Martín, P. Ávila, S.S. Suárez, M. Yates, A.B. Martín-Rojo, C. Barthelemy, J.A. Martín, Appl. Catal. B: Environ. 67 (2006) 270–278.
[13] C.H. He, M. Paulus, W. Chu, J. Find, J.A. Nickl, K. Köhler, Catal. Today 131 (2008) 305–313.

[14] L.F. Liotta, G. Pantaleo, G.D. Carlo, G. Marcì, G. Deganello, Appl. Catal. B: Environ. 52 (2004) 1–10.
[15] D. Pietrogiacomi, M.C. Campa, S. Tuti, V. Indovina, Appl. Catal. B: Environ. 41 (2003) 301–312.
[16] V. Indovina, D. Pietrogiacomi, M.C. Campa, J. Mol. Catal. A: Chem. 204–205 (2003) 655–662.
[17] M. Kantcheva, A.S. Vakkasoglu, J. Catal. 223 (2004) 352–363.
[18] M. Kantcheva, A.S. Vakkasoglu, J. Catal. 223 (2004) 364–371.
[19] S.K. Bhargava, D.B. Akolekar, J. Colloid Interface Sci. 281 (2005) 171–178.
[20] V.G. Milt, M.A. Ulla, E.E. MirÓ, Appl. Catal. B: Environ. 57 (2005) 13–21.
[21] M. Haneda, Y. Kintaichi, N. Bion, H. Hamada, Appl. Catal. B: Environ. 46 (2003) 473–482.
[22] X. Li, C.B. Zhang, H. He, Y. Teraoka, Appl. Catal. B: Environ. 75 (2007) 167–174.
[23] Z.L. Zhang, H.R. Geng, L. Zheng, B. Du, J. Alloys Compd. 392 (2005) 317–321.
[24] S. Iwamoto, R. Takahashi, M. Inoue, Appl. Catal. B: Environ. 70 (2007) 146–150.
[25] M. Haneda, Y. Kintaichi, H. Hamada, Appl. Catal. B: Environ. 55 (2005) 169–175.
[26] K. Asano, C. Ohnishi, S. Iwamoto, Y. Shioya, M. Inoue, Appl. Catal. B: Environ. 78 (2008) 242–249.
[27] H.Q. Wan, Z. Wang, J. Zhu, X.W. Li, B. Liu, F. Gao, L. Dong, Y. Chen, Appl. Catal. B: Environ. 79 (2008) 254–261.
[28] Y.H. Hu, L. Dong, M.M. Shen, D. Liu, J. Wang, W.P. Ding, Y. Chen, Appl. Catal. B: Environ. 31 (2001) 61–69.
[29] X.W. Li, M.M. Shen, X. Hong, H. Zhu, F. Gao, Y. Kong, L. Dong, Y. Chen, J. Phys. Chem. B 109 (2005) 3949–3955.
[30] H.L. Chen, H.Y. Zhu, Y. Wu, F. Gao, L. Dong, J. Zhu, J. Mol. Catal. A: Chem. 255 (2006) 254–259.
[31] T. He, D. Chen, X.L. Jiao, Chem. Mater. 16 (2004) 737–743.
[32] I. Lopes, N.E. Hassan, H. Guerba, G. Walllez, A. Davidson, Chem. Mater. 18 (2006) 5826–5828.
[33] G.S. Qi, R.T. Yang, Appl. Caral. B: Environ. 51 (2004) 93–106.
[34] A.W. Aylor, S.C. Larsen, J.A. Reimer, A.T. Bell, J. Catal. 157 (1995) 592–602.
[35] Y.F. Chang, J.G. McCarty, J. Catal. 165 (1997) 1–11.
[36] T. Taniike, M. Tada, R. Coquet, Y. Morikawa, T. Sasaki, Y. Iwasawa, Chem. Phys. Lett. 443 (2007) 66–70.
[37] C.M. Kim, C.W. Yi, D.W. Goodman, J. Phys. Chem. B 106 (2002) 7065–7068.
[38] I. Spassova, M. Khristova, R. Nickolov, D. Mehandjiev, J. Colloid Interface Sci. 320 (2008) 186–193.
[39] J.S. Shu, W.S. Xia, Y.J. Zhang, T. Cheng, M.R. Gao, Chin. J. Chem. Phys. 21 (2008) 383–400.
[40] D. Stoyanova, M. Christova, P. Dimitrova, J. Marinova, N. Kasabova, D. Panayotov, Appl. Catal. B: Environ. 17 (1998) 233–244.
[41] D. Panayotov, M. Christova, M. Velikova, Appl. Catal. B: Environ. 9 (1996) 107–132.
[42] J. Fan, X.D. Wu, X.D. Wu, Q. Liang, R. Ran, D. Weng, Appl. Catal. B: Environ. 81 (2008) 38–48.
[43] H. Vidal, J. Kašpar, M. Pijolat, G. Colon, S. Bernal, A. Cordón, V. Perrichon, F. Fally, Appl. Catal. B: Environ. 27 (2000) 49–63.
[44] B. Azambre, L. Zenboury, F. Delacroix, J.V. Weber, Catal. Today 137 (2008) 278–282.